A&A 455, 291–301 (2006)
DOI: 10.1051/0004-6361:20065209


Astronomy & Astrophysics

# First stars IX - Mixing in extremely metal-poor giants. Variation of the $^{12}C/^{13}C$, [Na/Mg] and [Al/Mg] ratios⋆

M. Spite[1], R. Cayrel[1], V. Hill[1], F. Spite[1], P. François[1], B. Plez[2], P. Bonifacio[1], P. Molaro[1,4], E. Depagne[3], J. Andersen[7,8], B. Barbuy[5], T. C. Beers[6], B. Nordström[7,9], and F. Primas[10]

[1] GEPI, Observatoire de Paris-Meudon, 92125 Meudon Cedex, France
e-mail: monique.spite@obspm.fr
[2] GRAAL, Université de Montpellier II, 34095 Montpellier Cedex 05, France
[3] European Southern Observatory (ESO), Casilla 19001, Santiago 19, Chile
[4] Osservatorio Astronomico di Trieste, INAF, via G.B. Tiepolo 11, 34131 Trieste, Italy
[5] IAG, Universidade de Sao Paulo, Depto. de Astronomia, Rua do Matao 1226, Sao Paulo 05508-900, Brazil
[6] Department of Physics & Astronomy, CSCE: Center for the Study of Cosmic Evolution, and JINA: Joint Institute for Nuclear Astrophysics, Michigan State University, East Lansing, MI 48824, USA
[7] The Niels Bohr Institute, Astronomy, Juliane Maries Vej 30, 2100 Copenhagen, Denmark
[8] Nordic Optical Telescope Scientific Association, Apartado 474, 38 700 Santa Cruz de La Palma, Spain
[9] Lund Observatory, Box 43, 221 00 Lund, Sweden
[10] European Southern Observatory, Karl Schwarzschild-Str. 2, 85749 Garching bei München, Germany

Received 15 March 2006 / Accepted 19 April 2006

**ABSTRACT**

*Context.* Extremely metal-poor (EMP) stars preserve a fossil record of the composition of the ISM when the Galaxy formed. It is crucial, however, to verify whether internal mixing has modified their surface composition, especially in the giants where most elements can be studied.
*Aims.* We aim to understand the CNO abundance variations found in some, but not all EMP field giants analysed earlier. Mixing beyond the first dredge-up of standard models is required, and its origin needs clarification.
*Methods.* The $^{12}C/^{13}C$ ratio is the most robust diagnostic of deep mixing, because it is insensitive to the adopted stellar parameters and should be uniformly high in near-primordial gas. We have measured $^{12}C$ and $^{13}C$ abundances in 35 EMP giants (including 22 with [Fe/H] $< -3.0$) from high-quality VLT/UVES spectra analysed with LTE model atmospheres. Correlations with other abundance data are used to study the depth of mixing.
*Results.* The $^{12}C/^{13}C$ ratio is found to correlate with [C/Fe] (and Li/H), and clearly anti-correlate with [N/Fe], as expected if the surface abundances are modified by CNO processed material from the interior. Evidence for such deep mixing is observed in giants above $\log L/L_{\odot} = 2.6$, brighter than in less metal-poor stars, but matching the bump in the luminosity function in both cases. Three of the mixed stars are also Na- and Al-rich, another signature of deep mixing, but signatures of the ON cycle are not clearly seen in these stars.
*Conclusions.* Extra mixing processes clearly occur in luminous RGB stars. They cannot be explained by standard convection, nor in a simple way by rotating models. The Na- and Al-rich giants could be AGB stars themselves, but an inhomogeneous early ISM or pollution from a binary companion remain possible alternatives.

**Key words.** Galaxy: abundances – Galaxy: evolution – stars: abundances – stars: interiors – stars: supernovae: general – stars: evolution

## 1. Introduction

The surface composition of a cool star is a good diagnostic of the chemical composition of the gas from which it formed, if mixing with material processed inside the star itself has not occurred. We are conducting a comprehensive spectroscopic study of extremely metal-poor (EMP) stars to obtain precise and detailed information on the chemical composition of the ISM in the early Galaxy and the yields of the first generation(s) of supernovae. Using the ESO VLT and UVES spectrograph, we have obtained abundance results of unprecedented quality for a large sample of faint halo stars. The next step is to investigate to what extent these abundances represent the composition of the early ISM.

The most complete range of elements can be studied in the cool, low-gravity atmospheres of red giant stars. Accordingly, Cayrel et al. (2004, "First Stars V") determined abundances for the elements from C to Zn in a sample of 35 EMP giants. 30 of the stars were found to have $-4.1 <$ [Fe/H] $< -2.7$, while 22 stars have [Fe/H] $\leqslant -3.0$. Very tight abundance relations were found for nearly all elements, with C and N as notable exceptions. As C, N, and O are the first elements synthesised after the Big Bang, their abundances in the early galactic gas are of particular interest and merit further study.

In a subsequent paper (Spite et al. 2005, "First Stars VI"), we found the C and N abundances in our sample to be anti-correlated. Two groups of stars were clearly separated in a plot

⋆ Based on observations obtained with the ESO Very Large Telescope at Paranal Observatory, Chile (Large Programme "First Stars", ID 165.N-0276(A); P.I.: R. Cayrel).

of [N/Fe] vs. [C/Fe]: A first group, named "unmixed" stars had [N/Fe] < 0.5, [C/Fe] > 0.0, and measurable Li abundances in the range $0.2 < A(\mathrm{Li}) < 1.2$, while a second group of "mixed" stars had [N/Fe] > 0.5, [C/Fe] < 0.0, and Li below our detection threshold. However, [(C+N)/Fe] was practically identical in the two subsamples. We also found the "unmixed" stars to lie mostly on the lower part of the Red Giant Branch (RGB), while the "mixed" stars seemed to lie on the upper RGB or even the Horizontal Branch (HB) or asymptotic giant branch (AGB). Let us remark here that the adjectives "mixed" and "unmixed", as defined in our paper "First Stars VI", may appear a bit misleading. All of the stars studied in these papers are giants, and thus they all have undergone the first dredge-up. This can be clearly seen from the abundance of lithium, which is close to $A(\mathrm{Li}) = 2.3$ in EMP dwarfs (Bonifacio et al. 2006, "First Stars VII") and is only $A(\mathrm{Li}) < 1.2$ in our sample of giants (see "First Stars VI"). Lithium is a very fragile element, and mixing with layers at temperatures higher than only $2.5 \times 10^6$ K is able to destroy it. As a first approximation, we can suppose that the first dredge-up does not affect the abundances of the elements heavier than Li in low-mass stars ($\mathscr{M}/\mathscr{M}_\odot \leq 0.9$). The effect on [C/Fe] and [N/Fe], following, e.g., Gratton et al. (2000) or Denissenkov & Weiss (2004) is negligeable. In "First stars VI", and in this paper we use the term "mixed stars" only for stars that have undergone mixing with deep layers of the star, thereby affecting the observed CNO abundances, and "unmixed" stars for those which such deep mixing is not expected to have occured.

The simplest explanation of the observed C and N abundances is that mixing has occurred between the atmosphere of the upper RGB stars and the H-burning layer where C is converted into N by the CNO cycle (e.g. Charbonnel 1995). Evidence for mixing in upper RGB stars has already been observed in globular cluster giants (Kraft 1994; Bellman et al. 2001; Shetrone 2003; Grundahl et al. 2002), open clusters (Gilroy 1989; Jacobson et al. 2005), and field giants (Shetrone et al. 1993; Charbonnel et al. 1998; Gratton et al. 2000). However, these stars were only moderately metal-poor ($-2 <$ [Fe/H] $< -0.5$), substantially more metal-rich than our present sample.

Convection, the only mechanism of internal mixing in "standard models", cannot by itself account for these observations. Different models have been proposed to explain the observed extra mixing (e.g. Denissenkov & VandenBerg 2003; Chanamé et al. 2005; Palacios et al. 2006) and predict that mixing should be a function of metallicity: at any given depth in a stellar interior, a metal-poor star is hotter than a metal-rich star of the same mass; thus, the CN and ON processing shells are closer to the surface, facilitating mixing (Charbonnel 1994; Charbonnel et al. 1998). However, Gratton et al. (2000) note that, in their sample of moderately metal-poor stars, mixing apparently reaches a maximum for stars with [Fe/H] $\approx -1.5$.

The primary aim of the present paper is to better constrain the models of internal mixing in giant stars, especially in EMP giants. Measurements of the $^{12}C/^{13}C$ ratio are a particularly powerful tool, because $^{12}C/^{13}C$ is largely unaffected by uncertainties in the adopted stellar parameters, and appears to be high (>70) in nearly primordial gas (e.g. Levshakov et al. 2005). As a result, any significant variation of $^{12}C/^{13}C$ should be due to internal mixing processes in the stars.

## 2. Observations and reduction

The observations were performed with the ESO VLT and its high-resolution spectrograph UVES (Dekker et al. 2000). Briefly, the spectra have a resolution of $R = 47\,000$ at $\lambda = 400$ nm and typical S/N ratios per pixel of ~130, with an average of 5 pixels per resolution element; they were reduced using the UVES context within MIDAS (Ballester et al. 2000). Our spectra and their reduction are described in detail by Cayrel et al. (2004, "First Stars V"); sample spectra of the region of interest in this paper are shown in Fig. 1.

## 3. Analysis

We have carried out a classical LTE analysis using OSMARCS models (see, e.g., Gustafsson et al. 1975, 2003). $T_{\rm eff}$ was derived from photometry, using the calibration of Alonso et al. 1999, and $\log g$ from the ionisation equilibrium of Fe and Ti. Microturbulent velocities were fixed by requiring no trend of [Fe I/H] with equivalent width. Details of the analysis are given in "First Stars V".

The C abundance and $^{12}C/^{13}C$ ratio were determined by spectrum synthesis of the $A^2\Delta - X^2\Pi$ band of CH (the G band), using the current version of the Turbospectrum code (Alvarez & Plez 1998). The CH line positions were computed with the program LIFBASE (Luque & Crosley 1999), and $gf$ values, excitation energies, and isotopic shifts were taken from the line list of Jørgensen et al. (1996). Several features of the band were used, but the stronger lines of $^{13}C$ are at 423.030, 423.145, and 423.655 nm, respectively. Sample spectrum fits are shown in Fig. 1.

We note that the $^{13}C$ line at 423.030 nm is sometimes blended by an unidentified line, probably due to an *r*-process element. In the extreme *r*- process-element rich giant CS 31082-001 (Hill et al. 2002, "First Stars I"), this line is quite strong (Fig. 1), and it may contribute significantly to the $^{13}C$ feature in other *r*-process enhanced EMP giants. Alternative regions of the spectra of r-process-rich stars, such as the near-IR, might be usefully explored for measurement of this species.

Table 1 lists the adopted parameters for our program stars as well as the derived N abundance (from "First Stars VI"), C abundance and $^{12}C/^{13}C$ ratios. Note that [C/H] as given in Table 1 refers to the total C abundance ($^{12}C + ^{13}C$). It may be slightly different from the values given in "First Stars VI", where [C/H] was derived from the $^{12}CH$ lines, assuming a solar $^{12}C/^{13}C$ ratio, but the maximum difference is less than 2%.

Deriving $^{13}C$ abundances in our very weak-lined EMP stars is a challenge, as the parent $^{12}CH$ lines are already quite weak. [C/H] is relatively high in the unmixed stars, but $^{13}C/^{12}C$ is then low and the $^{13}C$ lines weak. And while $^{13}C/^{12}C$ is higher in the mixed stars, [$^{12}$C/H] itself is low because some of the C has been transformed into N. As a result, the measurement errors given in Table 1 are relatively large; for eight stars we could not measure the $^{12}C/^{13}C$ ratio at all. In three of them (CD –38:245, BS 16467– 062, and CS 22952–015), [C/H] is so low that no parent $^{12}CH$ lines are visible in the region of the $^{13}CH$ lines. For the five other stars, the measured upper limit of $^{12}C/^{13}C$ is not very useful ($^{12}C/^{13}C > 5$).

Fortunately, uncertainties in the physical parameters of the stars do not significantly affect the resulting $^{12}C/^{13}C$ ratio: differences in $T_{\rm eff}$, $\log g$, and even microturbulent velocity affect the $^{12}CH$ and $^{13}CH$ molecules nearly identically, especially when the lines are of similar strength and/or not saturated, as in our EMP giants (see, e.g., Sneden et al. 1986). 3D effects should also be unimportant for the isotope ratio. Therefore, the errors of $^{12}C/^{13}C$ as given in Table 1 should reflect the total uncertainty in the isotope ratio.

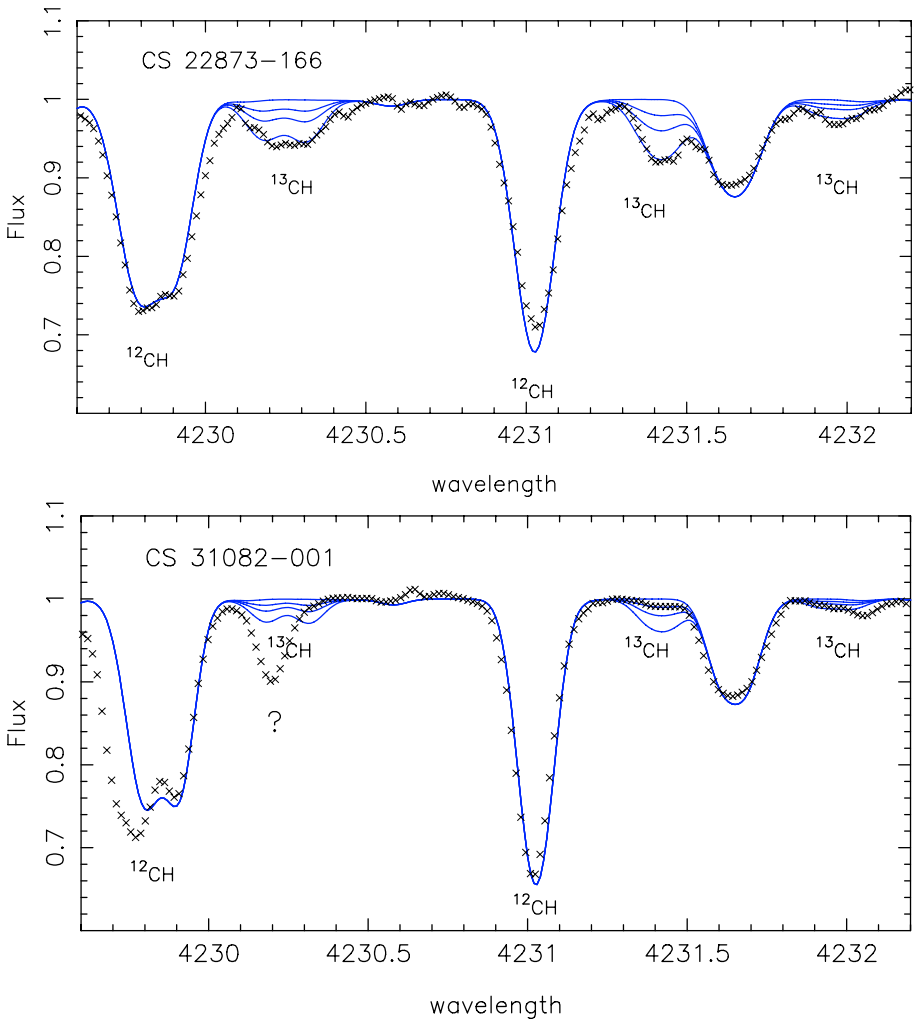


**Fig. 1.** Reduced UVES spectra (crosses) in the region of the $^{13}C$ features. Synthetic spectra are shown (full lines), computed without $^{13}C$ as well as for $\log {}^{12}C/{}^{13}C$ = 1.3 1.0 0.7 for CS 22873-166, $\log {}^{12}C/{}^{13}C$ = 1.6 1.3 1.0 for CS 31082-001. The best fits are for $\log {}^{12}C/{}^{13}C$ = 0.7 ($^{12}C/^{13}C$ = 5) in CS 22873-166 and $\log {}^{12}C/{}^{13}C$ = 1.6 ($^{12}C/^{13}C$ = 40) in CS 31082-001. The $^{13}C$ line at 4230.3 Å in CS 31082-001 is severely blended by an unidentified line, probably due to an *r*-process element, as these elements are strongly enhanced in this star (Hill et al. 2002).

Two of our EMP giants are "C-rich" (Table 1, last column); see Depagne et al. (2002) and Sneden et al. (2000, 2003). These very peculiar stars are omitted in the following discussion.

In "First Stars I", we found $^{12}C/^{13}C > 20$ for CS 31082-001, but the additional spectra obtained by Plez et al. (2004) permit us to tighten this upper limit: $^{12}C/^{13}C > 30$. Unfortunately, in CS 31082-001 the accuracy of the determination is affected by an unidentified line blending with the strongest $^{13}C$ line (see Fig. 1 and the text above).

In Fig. 2 we show the $^{12}C/^{13}C$ ratio vs. $T_{\rm eff}$ and $\log g$ for our sample of EMP giants. Clearly, all the stars found to belong to the mixed subsample in "First Stars VI" (Spite et al. 2005) have a low $^{12}C/^{13}C$ ratio.

In general, we found the unmixed giants to lie on the lower RGB, while the mixed giants are on the HB or upper RGB. However, CS 29518-051 seems to belong to the low RGB ($T_{\rm eff}$ = 5200, $\log g$ = 2.6; see Fig. 5), although we find it exhibits the characteristically high [N/H] and low [C/H] and $A$(Li) of mixed giants ("First Stars VI"). CS 29518-051 also has a very low $^{12}C/^{13}C$ ratio, confirming that its atmosphere has been mixed with CNO-processed matter. Since a large error in $\log g$ of this star is unlikely, it would be interesting to monitor its radial velocity to verify whether it may have been polluted by a binary companion. As an alternative, CS 29518-051 could be a horizontal-branch star (see Sect. 4.1).

### 3.1. Correlations between $^{12}C/^{13}C$ and the C and N abundances

Figures 3a,b show $^{12}C/^{13}C$ vs. [C/Fe] and [N/Fe] for our stars (Table 1). As seen, $^{12}C/^{13}C$ increases steeply with [C/Fe] and decreases as [N/Fe] increases. Moreover, we find $\log (^{12}C/^{13}C) \approx 0.7$ at the lowest [C/N] ratios (i.e., most complete processing), close to the equilibrium ratio for the CNO process.

The star CS 29516-024 has a rather low C abundance for an unmixed star (Fig. 3a), but it also has the lowest [N/Fe] in our sample (Fig. 3a), resulting in a normal [C/N] ratio (Fig. 3c). Its relatively high $^{12}C/^{13}C$ = 20 (Figs. 3a–c) indicates that any mixing of the atmosphere with deeper layers has not been very important, so the gas that formed this star should have had the observed low N abundance, or perhaps even lower.

The effects of mixing with CNO processed material are illustrated in Fig. 3c. The curves show the relations between $^{12}C/^{13}C$ and [C/N] that result when a stellar atmosphere is progressively mixed with material in which 80% (full line) or 90% (dashed) of the initial C has been burned into N. Note that the three leftmost stars in Fig. 3c (CS 22873–055, CS 22878–101, and CS 22891–209) have lower [C/N] ratios than most of the other mixed stars, which can be understood in terms of mixing with nearly fully CNO processed material (dashed line). CS 22952-015 should be added to this list, as it exhibits the lowest C abundance and [C/N] ratio in the sample; unfortunately, its C abundance is too low to

**Table 1.** Adopted model atmosphere parameters ($T_{\rm eff}$, log $g$, $v_{\rm t}$, [Fe/H]), C and N abundances, and $^{12}C/^{13}C$ ratios for the programme stars. [C/H], as given in this table, is the sum [($^{12}C$ +$^{13}$ C)/H]. An "m" in the "Mix" column denotes the "mixed" stars. The two "C -rich" stars are very peculiar and are omitted from the figures and the discussion. (Owing to some improvements the values in this table maybe slightly different from the values given in Paper VI.)

| | Star | $T_{\rm eff}$ | log $g$ | $v_{\rm t}$ | [Fe/H] | log $L/L_\odot$ | [C/H] | [N/H] | [(C+N)/H] | [C/N] | $^{12}C/^{13}C$ | mix. | Rem. |
|---|---|---|---|---|---|---|---|---|---|---|---|---|---|
| 1 | HD 2796 | 4950 | 1.5 | 2.1 | −2.47 | 2.60 | −2.87 ± 0.06 | −1.62 ± 0.08 | −2.23 | −1.25 | 4 ± 2 | m | |
| 2 | HD 122563 | 4600 | 1.1 | 2.0 | −2.82 | 2.87 | −3.21 ± 0.05 | −2.12 ± 0.15 | −2.70 | −1.09 | 5 ± 2 | m | |
| 3 | HD 186478 | 4700 | 1.3 | 2.0 | −2.59 | 2.71 | −2.81 ± 0.07 | −1.97 ± 0.12 | −2.47 | −0.84 | 5 ± 2 | m | |
| 4 | BD +17:3248 | 5250 | 1.4 | 1.5 | −2.07 | 2.80 | −2.40 ± 0.05 | −1.42 ± 0.10 | −1.97 | −0.98 | 10 ± 5 | m | |
| 5 | BD –18:5550 | 4750 | 1.4 | 1.8 | −3.06 | 2.63 | −3.08 ± 0.04 | −3.42 ± 0.10 | −3.13 | +0.34 | >40 | | |
| 6 | CD –38:245 | 4800 | 1.5 | 2.2 | −4.19 | 2.55 | <− 4.52 | −3.12 ± 0.20 | <− 3.75 | <− 1.40 | − | m | |
| 7 | BS 16467–062 | 5200 | 2.5 | 1.6 | −3.77 | 1.69 | −3.52 ± 0.12 | <− 3.32 | <− 3.47 | >−0.20 | − | | |
| 8 | BS 16477–003 | 4900 | 1.7 | 1.8 | -3.36 | 2.38 | −3.07 ± 0.08 | <− 3.62 | <− 3.14 | >+ 0.55 | >30 | | |
| 9 | BS 17569–049 | 4700 | 1.2 | 1.9 | −2.88 | 2.81 | −2.93 ± 0.05 | −2.02 ± 0.12 | −2.54 | −0.91 | 6 ± 2 | m | |
| 10 | CS 22169–035 | 4700 | 1.2 | 2.2 | −3.04 | 2.81 | −3.20 ± 0.05 | −2.02 ± 0.13 | −2.62 | −1.18 | 6.5 ± 2 | m | |
| 11 | CS 22172–002 | 4800 | 1.3 | 2.2 | −3.86 | 2.75 | −3.86 ± 0.10 | −3.62 ± 0.20 | −3.80 | −0.24 | >10 | | |
| 12 | CS 22186–025 | 4900 | 1.5 | 2.0 | −3.00 | 2.58 | −3.54 ± 0.10 | −2.02 ± 0.08 | −2.67 | −1.52 | − | m | |
| 13 | CS 22189–009 | 4900 | 1.7 | 1.9 | −3.49 | 2.38 | −3.15 ± 0.08 | −3.22 ± 0.12 | −3.16 | +0.07 | 15 (+8 −5) | | |
| 14 | CS 22873–055 | 4550 | 0.7 | 2.2 | −2.99 | 3.25 | −3.62 ± 0.06 | −1.92 ± 0.20 | −2.58 | -1.70 | 4 ± 2 | m | Na-rich |
| 15 | CS 22873–166 | 4550 | 0.9 | 2.1 | −2.97 | 3.05 | −3.10 ± 0.08 | −1.92 ± 0.20 | −2.52 | −1.18 | 5 ± 2 | m | |
| 16 | CS 22878–101 | 4800 | 1.3 | 2.0 | −3.25 | 2.75 | −3.46 ± 0.10 | −1.92 ± 0.10 | −2.57 | −1.54 | 5 ± 2 | m | |
| 17 | CS 22885–096 | 5050 | 2.6 | 1.8 | −3.78 | 1.53 | −3.52 ± 0.06 | −3.52 ± 0.13 | −3.52 | 0.00 | − | | |
| 18 | CS 22891–209 | 4700 | 1.0 | 2.1 | −3.29 | 3.01 | −3.86 ± 0.05 | −2.17 ± 0.10 | −2.83 | −1.69 | 5 ± 2 | m | Na-rich |
| 19 | CS 22892–052 | 4850 | 1.6 | 1.9 | −3.03 | 2.46 | −2.11 ± 0.06 | −2.52 ± 0.13 | −2.17 | +0.41 | 16 (+8 −5) | | C-rich |
| 20 | CS 22896–154 | 5250 | 2.7 | 1.2 | −2.69 | 1.50 | −2.46 ± 0.05 | −2.92 ± 0.12 | −2.52 | +0.46 | >40 | | |
| 21 | CS 22897–008 | 4900 | 1.7 | 2.0 | −3.41 | 2.38 | −2.83 ± 0.05 | −3.17 ± 0.15 | −2.88 | +0.34 | 20 (+8 −5) | | |
| 22 | CS 22948–066 | 5100 | 1.8 | 2.0 | −3.14 | 2.35 | −3.06 ± 0.10 | −1.92 ± 0.10 | −2.51 | −1.14 | − | m | |
| 23 | CS 22949–037 | 4900 | 1.5 | 1.8 | −3.97 | 2.58 | −2.72 ± 0.10 | −1.72 ± 0.30 | −2.27 | −1.00 | 4 ± 2 | m | C-rich |
| 24 | CS 22952–015 | 4800 | 1.3 | 2.1 | −3.43 | 2.75 | −4.02 ± 0.08 | −2.12 ± 0.10 | −2.80 | −1.90 | − | m | Na-rich |
| 25 | CS 22953–003 | 5100 | 2.3 | 1.7 | −2.84 | 1.85 | −2.52 ± 0.03 | −2.72 ± 0.10 | −2.55 | +0.20 | 20 (+8 −5) | | |
| 26 | CS 22956–050 | 4900 | 1.7 | 1.8 | −3.33 | 2.38 | −3.06 ± 0.05 | −3.02 ± 0.10 | −3.05 | −0.04 | − | | |
| 27 | CS 22966–057 | 5300 | 2.2 | 1.4 | −2.62 | 2.02 | −2.56 ± 0.05 | −2.52 ± 0.12 | −2.55 | −0.04 | − | | |
| 28 | CS 22968–014 | 4850 | 1.7 | 1.9 | −3.56 | 2.36 | −3.30 ± 0.06 | −3.32 ± 0.10 | −3.30 | +0.02 | 30 (+8 −5) | | |
| 29 | CS 29491–053 | 4700 | 1.3 | 2.0 | −3.04 | 2.71 | −3.25 ± 0.05 | −2.22 ± 0.15 | −2.78 | −1.03 | 7 ± 2 | m | |
| 30 | CS 29495–041 | 4800 | 1.5 | 1.8 | −2.82 | 2.55 | −2.86 ± 0.06 | −2.42 ± 0.10 | −2.73 | −0.44 | 14 (+8 −5) | | |
| 31 | CS 29502–042 | 5100 | 2.5 | 1.5 | -3.19 | 1.65 | −3.03 ± 0.04 | −3.62 ± 0.20 | −3.10 | +0.59 | >30 | | |
| 32 | CS 29516–024 | 4650 | 1.2 | 1.7 | −3.06 | 2.79 | −3.10 ± 0.05 | −3.82 ± 0.20 | −3.18 | +0.72 | 20 (+8 -5) | | |
| 33 | CS 29518–051 | 5200 | 2.6 | 1.4 | −2.69 | 1.59 | −2.77 ± 0.05 | −1.87 ± 0.15 | −2.39 | −0.90 | 8 ± 2 | m | |
| 34 | CS 30325–094 | 4950 | 2.0 | 1.5 | −3.30 | 2.10 | −3.28 ± 0.05 | −3.12 ± 0.18 | −3.24 | −0.16 | 20 (+8 −5) | | |
| 35 | CS 31082–001 | 4825 | 1.5 | 1.8 | −2.91 | 2.56 | −2.68 ± 0.05 | −3.42 ± 0.10 | −2.76 | +0.74 | >30 | | |

yield a usable $^{12}C/^{13}C$ ratio, so it is not shown in the figures. Most of these stars are found below (see Sect. 4.3.1) to also show enhanced Na and Al abundances.

### 3.2. $^{12}C/^{13}C$ ratios vs. Li abundances

Figure 4 shows log$^{12}C/^{13}C$ as a function of $A$(Li) for our sample of unmixed giants. $A$(Li) = log $\varepsilon$(Li), is the logarithm of the number of Li atoms per $10^{12}$ H atoms. In the mixed giants the Li line is too weak to be measured ($A$(Li) < 0.0), but $^{12}C/^{13}C \approx 5.0 \pm 2$; all these stars fall in the hatched part of the diagram. During the evolution of a star, $A$(Li) decreases as the $^{13}C$ abundance increases and $^{12}C/^{13}C$ gradually declines towards the CNO equilibrium value. Thus, the mixing process involves the whole stellar envelope, bringing CNO processed material to the surface layers while simultaneously depleting Li.

## 4. Discussion

### 4.1. The bump luminosity in metal-poor stars

Our EMP stars are too faint to have been observed by Hipparcos, so no accurate direct distance and luminosity determinations are available for them. Meanwhile, we can estimate luminosities from their atmospheric parameters via the classical formula:

$$\log\ L/L_\odot = \log\ \mathscr{M}/\mathscr{M}_\odot + 4\ \log\ T_{\rm eff}/T_{\rm eff,\odot} - \log\ g/g_\odot$$

with $T_{\rm eff,\odot}$ = 5780 K, log $g_\odot$ = 4.44 and assuming all of the stars have a mass $\mathscr{M} = 0.85\mathscr{M}_\odot$.

For the EMP giants, we take $T_{\rm eff}$ and log $g$ from "First Stars V", for the turnoff stars from Bonifacio et al. (2006, "First Stars VII"). The resulting luminosities are listed in Table 1. With errors of 100 K in $T_{\rm eff}$ and 0.2 dex in log $g$ (see "First Stars V"), we estimate that $\Delta(\log\ L/L_\odot) \approx 0.2$ dex.

Figure 5 shows a comparison of our EMP giant and turnoff stars with the stars observed by Gratton et al. (2000); as expected, their moderately metal- poor stars (−2 < [Fe/H] < −1) are on average cooler than our stars. Fig. 5 also shows isochrones by Kim et al. (2002) for 14 Gyr, [$\alpha$/Fe] = +0.6, [Fe/H] = −3.7 (full line) and [Fe/H] = −2.7 (dashed line). For comparison, the dotted line shows an isochrone corresponding to the Gratton et al. stars (12 Gyr, [$\alpha$/Fe] = +0.3, [Fe/H] = −1.5; also from Kim et al. 2002). The isochrones fit the data within the errors for both sets of RGB stars (the unmixed giant CS 22966-057 seems to be overluminous for its $T_{\rm eff}$ hence it may be a binary; see "First Stars VI").

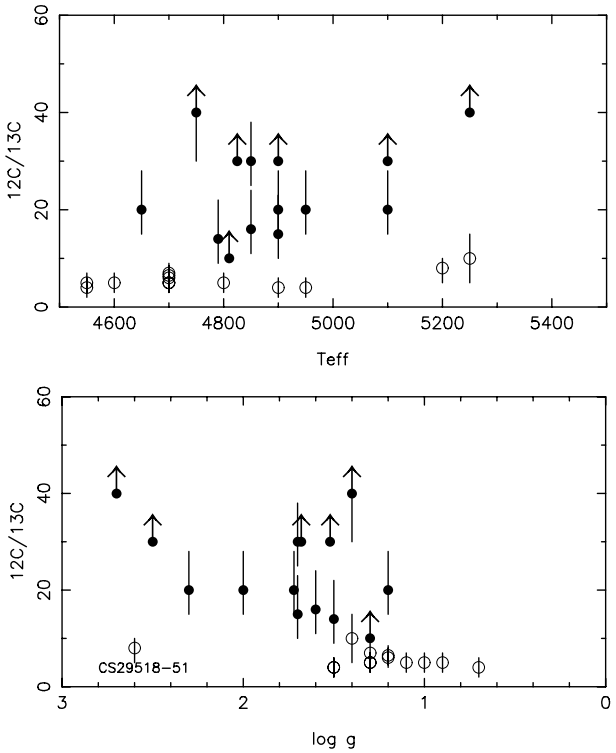


**Fig. 2.** $^{12}C/^{13}C$ vs. Teff and log g for our sample of EMP giants. Open and filled symbols denote "mixed" and "unmixed" stars, respectively (see "First Stars VI"). The lower $^{12}C/^{13}C$ ratios seen at lower log $g$ (i.e., higher luminosity) suggest extra mixing. Errors are about 100 K in $T_{\rm eff}$ and 0.2 dex in log $g$.

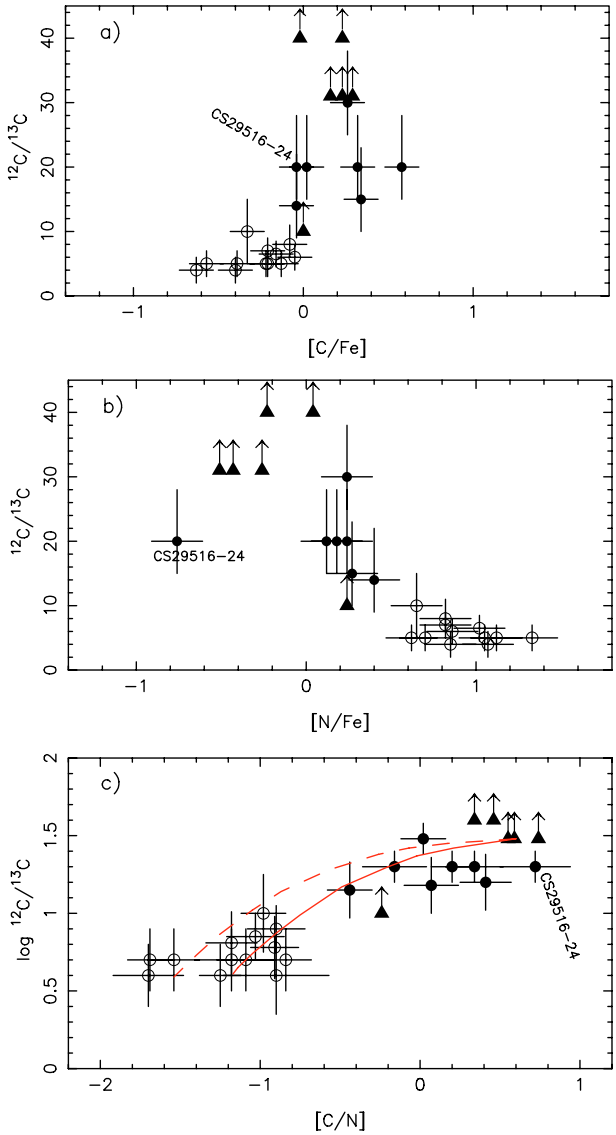


**Fig. 3. a)** $^{12}C/^{13}C$ vs. [C/Fe], **b)** vs. [N/Fe], and **c)** log$^{12}C/^{13}C$ vs. [C/N] for our sample of EMP giants. Symbols are as in Fig. 2; triangles denote upper limits. The correlation of $^{12}C/^{13}C$ with [C/Fe] (panel **a)**) and anticorrelation with [N/Fe] (panel **b)**) are well defined; both could be explained by extra mixing. The low N abundance of CS 29516-024 presumably reflects the composition of the ISM from which it formed. The gap in [C/N] used to separate the mixed and unmixed groups of stars is clearly visible in panel **c)**, but a small gap also appears within the mixed group, at [C/N] ~ −1.4; the stars with the lowest [C/N] values are also Na- and Al-rich (see Sect. 4.3.1 and Fig. 9). The curves show the computed evolution of log$^{12}C/^{13}C$ as a function of [C/N] in a stellar atmosphere progressively mixed with material in which 80% (full line) and 90% (dashed) of the C has been transformed into N by the CNO cycle.

As already noted by Denissenkov & VandenBerg (2003), the dwarfs of Gratton et al. (2000) appear to be shifted toward lower temperature, although their mean metallicity is similar to that of the giants. A similar, but smaller, effect is seen for our EMP turnoff stars, which tend to fall redward of the isochrone for [Fe/H] = −2.7. Following Denissenkov & VandenBerg, the most likely cause is a mismatch between the theoretical and the observed $T_{\rm eff}$ scales (see on this point Meléndez et al. 2006).

Gratton et al. (2000, their Fig. 7) found all of their luminous giants (above log $L/L_\odot \approx 1.8$) to show evidence of extra mixing between the surface and the H-burning layers, i.e.:

- very low Li abundance ($A$(Li) < 0.0);
- high N abundance and low [C/N] ratio;
- very low $^{12}C/^{13}C$ ratio.

The luminosity log $L/L_\odot \approx 1.8$ corresponds to the so-called "bump" in the luminosity function of the giants (LFB) in the sample of Gratton et al. (2000). At the LFB, the hydrogen burning shell inside the star crosses the H-profile discontinuity left behind by the base of the convective envelope during the first dredge-up, and the $\mu$ gradient barrier disappears, allowing the extra mixing to work.

The mixed stars in our sample present the same signatures (Li, C/N, $^{12}C/^{13}C$), and are identified in Fig. 5 by open circles; extra mixing clearly sets in at a higher luminosity in our more metal-poor EMP stars.

Theoretically, the luminosity of the LFB is expected to increase with decreasing metallicity (Charbonnel 1994). Denissenkov & VandenBerg (2003; their Fig. 1–2) give results for three metallicities: log $Z$ = −2.7, −3.0 and −3.3 ($Z$ = 0.002, 0.001, 0.0005) and $\mathcal{M}$ = 0.85$\mathcal{M}_\odot$. The bump luminosity appears to be an almost linear function of log $Z$; if we extrapolate it to the mean metallicity of our stars (log $Z$ = −4.52, $Z$ = 0.00003), we find the LFB to occur at log $L/L_\odot \approx 2.6$, corresponding well to the onset of mixing in our EMP stars. The link between the extra-mixing phenomenon and the bump thus seems to be well established.

Figure 5 shows that, surprisingly, one mixed star, CS 29518-051, is located well below the bump, very close to the horizontal branch as defined by the HB stars of Gratton et al. (2000). As the position of the HB depends only slightly on metallicity, CS 29518-051 could be in fact an HB star which has already

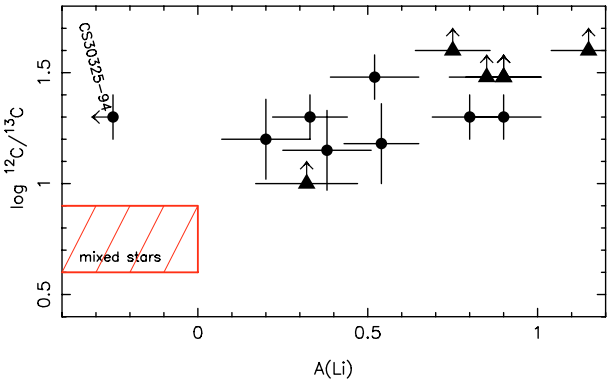


**Fig. 4.** $\log(^{12}C/^{13}C)$ vs. $A$(Li) (with $A$(Li) = $\log \varepsilon(Li)$); symbols as in Fig. 3. The dots are compatible with a linear relation between $\log ^{12}C/^{13}C$ and $A$(Li) for the unmixed stars in the interval $0.2 < A(\mathrm{Li}) < 1.2$. CS 30325- 94 is an unmixed star with an unusually low $A$(Li); see "First Stars VI". The very low lithium abundance $A$(Li) cannot be measured in the mixed stars, but the upper limits all fall in the hatched box in the diagram.

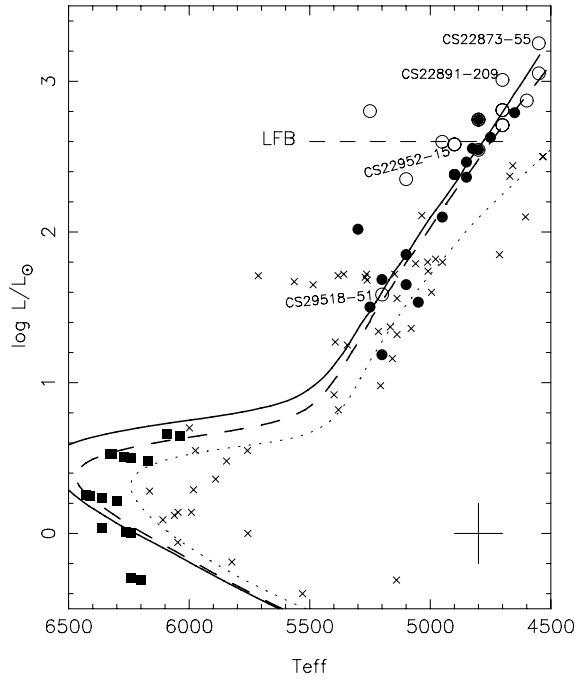


**Fig. 5.** H-R diagram for our EMP dwarfs (from "First Stars VII"; filled squares), unmixed giants (filled circles), and mixed giants (open circles). Crosses show the less metal-poor stars of Gratton et al. (2000). 14 Gyr isochrones by Kim et al. (2002) are shown for $[\alpha/\mathrm{Fe}] = +0.6$, $[\mathrm{Fe/H}] = -3.7$ (full line) and $[\mathrm{Fe/H}] = -2.7$ (dashed line); a 12 Gyr isochrone matching the Gratton et al. stars ($[\alpha/\mathrm{Fe}] = +0.3$, $[\mathrm{Fe/H}] = -1.5$) is included for comparison (dotted line). The horizontal dashed line at $\log L/L_\odot \approx 2.6$ indicates the luminosity function bump of the giants (LFB) for $[\mathrm{Fe/H}] \approx -3.2$ (extrapolated from Denissenkov & VandenBerg 2003). The three labelled stars at the top of the diagram are Na rich (Sect. 4.3). The mixed star CS 29518-051 could belong to the HB instead of the lower RGB (Sect. 3).

gone through the RGB bump as well as the helium core flash. Its abundances, typical of mixed stars, could be due to extra-mixing processes that occured during these phases. (Note that the HB was accidentally misplaced in Fig. 9 of "First Stars VI").

### 4.2. Comparison with models of stellar structure

The $\log ^{12}C/^{13}C$ ratio is a powerful tool for further tests of models of extra mixing in EMP stars, because it should depend only

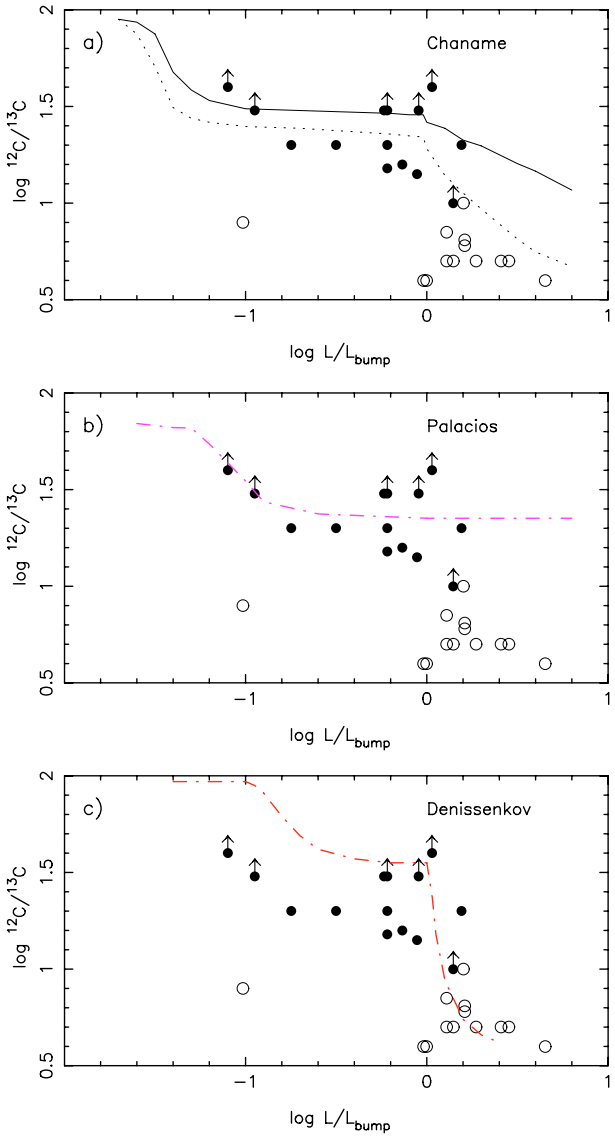


**Fig. 6.** $\log ^{12}C/^{13}C$ vs. $\log L/L_{\mathrm{bump}}$ in mixed and unmixed giants (symbols as in Fig. 2), compared to **a)** the predictions of Chanamé et al. (2005) for $[\mathrm{Fe/H}] = -1.4$ and $V_{TO} = 40$ km s$^{-1}$(full line) and 70 km s$^{-1}$(dotted line). **b)** the predictions of Palacios et al. (2006) which correspond to a value of $V_{TO}$ compatible to the observations ($\approx 4$ km s$^{-1}$). The rapid drop in $^{12}C/^{13}C$ would require very fast rotation speeds at the turnoff, incompatible with the observations. **c)** the predictions of Denissenkov & Weiss (2004). In this case the rapid drop in $^{12}C/^{13}C$ at the RGB bump is predicted. However, this model is essentially a standard model on top of which ad-hoc extra mixing is simulated.

on the internal mixing in the star and hardly at all on the composition of the near- primordial ISM from which the stars formed. By contrast, the atmospheric C and N abundances depend not only on internal mixing, but also on the initial C and N abundances, which may vary from star to star.

Figure 6 shows $\log ^{12}C/^{13}C$ as a function of $\log L/L_{\mathrm{bump}}$ for our stars. Clearly, as soon as a star reaches the bump luminosity, $^{12}C/^{13}C$ drops very abruptly. Two classes of models have been developed in order to account for these abundance changes:

– The first class of models are the "parametric diffusion models". Here, extra mixing is simulated by adding a diffusion

term to the equations that control the abundances of the different elements at different levels inside the stars (Boothroyd & Sackman 1999; Denissenkov & VandenBerg 2003).

– In the second class of models, the mechanism responsible for the extra mixing is associated with the transport of angular momentum in the stellar interior and modelled explicitly. Different mechanisms have been proposed, such as magnetic fields, gravity waves, and stellar rotation (see Charbonnel 1995; Chanamé et al. 2005; Palacios et al. 2006). Stellar rotation is often considered as the most promising non-standard mechanism to produce extra mixing, and its efficiency has been explored by Chanamé et al. (2005).

Unfortunately, the decline of $^{12}C/^{13}C$ along the RGB has only been modelled for metallicities above [Fe/H] $\approx -2$, a factor of 10 to 100 times higher than the stars we study here. In Fig. 6a we have compared our data with the predictions of Chanamé et al. (2005) for [Fe/H] $= -1.4$ and turnoff rotational velocities of 40 and 70 km s$^{-1}$. Neither of these values can explain the rapid drop in $^{12}C/^{13}C$ for log $L/L_{\rm bump} > 0$.

The best agreement is obtained with the higher rotational velocity, as has also been found when less metal-poor giants are compared with models. However, metal-poor field turnoff stars have rotational velocities less than 10 km s$^{-1}$ (see Lucatello & Gratton 2003).

The self-consistent models of Palacios et al. (2006) computed for [Fe/H] $= -1.6$ do not represent better the observations (these models correspond to rotational velocities at the turnoff compatible to the observations i.e. $\approx$4. km s$^{-1}$). In Fig. 6b we compare our observations to the predictions of the model M5 which gives the best fit, and none of the models predict a rapid decrease of the $^{12}C/^{13}C$ ratio after the bump.

So we conclude that if the observed mixed stars really *are* on the RGB, another extra-mixing process must be active. Note that Chanamé et al. and Palacios et al. have assumed solid rotation for the MS turnoff stars; if they have started their models from differentially rotating MS stars, the extra mixing (following Chanamé et al. (2005), would have been more vigorous for a given rotation rate.

In Sect. 3.2 we found that a good correlation exists between $^{12}C/^{13}C$ and $A$(Li). It is interesting to check whether the Li depletion in giants can also be explained by models. Figure 7a shows the Li depletion as a function of $T_{\rm eff}$, taking the initial ("plateau") Li abundance to be $A(\mathrm{Li})_0 = 2.2$ (thus $D(\mathrm{Li}) = A(\mathrm{Li}) - 2.2$). The unmixed stars, which have undergone the first dredge-up, are shown individually; in the mixed stars, we only have upper limits to $A$(Li), and these stars are located inside or below the hatched box.

The observational results are compared with theoretical Li depletion predictions following Charbonnel or Deliyannis (private communications to García Pérez & Primas 2006, see references therein), computed for stellar masses of 0.85 and 0.75 $M_\odot$, [Fe/H] $\approx -2$, and without extra-mixing. The agreement is rather good for $T_{\rm eff}$ higher than 5000 K, as the computed effect of the first dredge-up agrees with the observations; but at lower temperatures, i.e. higher luminosities, the Li abundance decreases more rapidly than predicted by the standard models.

In Fig. 7b the observed Li depletions are compared to the predictions of the self consistent models of Palacios et al. (2006): these models are not able to represent the rapid decrease of the lithium abundance after the bump; the computed effect of the rotation induced extra-mixing on the lithium abundance is negligible.

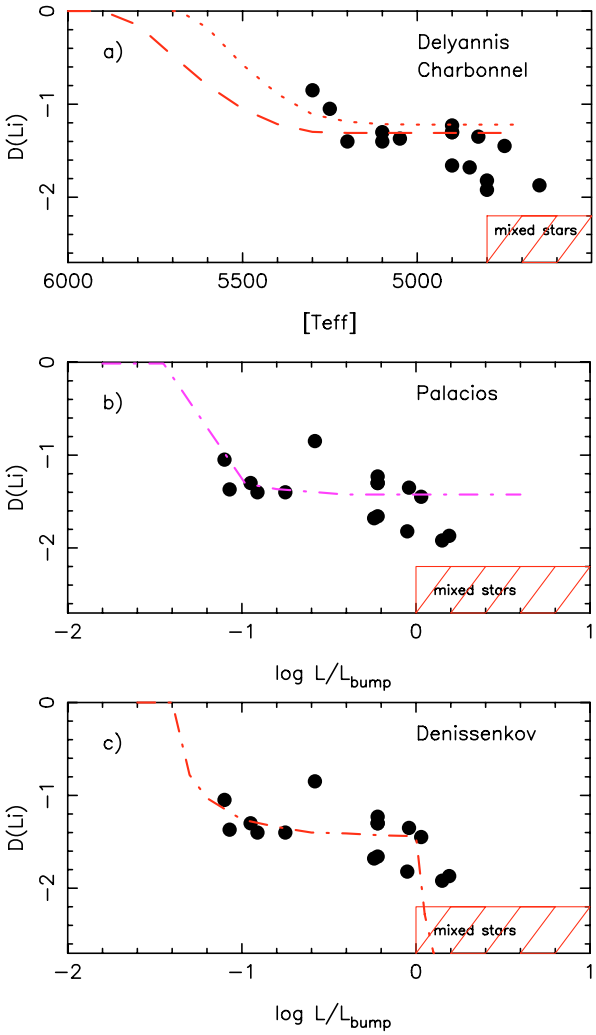


**Fig. 7.** Lithium depletions ($D$(Li) = $A$(Li) − 2.2) for our unmixed stars (dots), compared with model predictions. The hatched region contains the mixed RGB stars, for which $D$(Li) < −2.2. **a)** Models by Charbonnnel (dashed line) and Delyannis (dotted line), which do not include extra mixing. The observed Li depletion continues below 4900 K, at variance with the predictions. **b)** Self-consistent model (M5) of Palacios et al. (2006). **c)** Model by Denissenkov & Weiss (2004), which include extra mixing explicitly (see Fig. 6).

Finally in Fig. 7c the observed Li depletions are compared to the computations of Denissenkov & Weiss (2004), which explicitely include extra mixing. The agreement is rather good, but the parameters of the extra mixing (depth and rate) are ad-hoc and its cause (rotation, gravity waves . . . ) is not defined. Because the same parameters can explain the lithium abundances and the $^{12}C/^{13}C$ ratios, we can expect that extra mixing will be able to predict the abundances in the extremely metal-poor RGB stars once its phsyical cause is better understood.

For a better understanding of the mixing processes in the EMP giants, it would be important to extend the theoretical predictions of $^{12}C/^{13}C$ and D(Li) along the RGB to include stars with [Fe/H] $\leqslant -3.0$.

### *4.3. The mixed stars: RGB or AGB?*

So far, we have assumed that all our EMP giants lie on the RGB – the unmixed stars on the lower RGB, the mixed stars on the upper RGB (see "First Stars VI"). However, two facts advise

caution – the Na and Al abundances and excess luminosity of some of the stars. As Fig. 5 shows, some of the mixed stars are slightly more luminous than the theoretical RGB branch, and these might be AGB stars. Johnson (2002) also found that four among 23 metal-poor stars observed by her appeared to be AGB stars (as already noted by Bond 1980). In such stars, the core helium flash might perhaps induce extra mixing.

Gratton et al. (2000) observed several metal-poor horizontal branch (HB) stars, which have undergone the core helium flash. These stars exhibited the same characteristics as the mixed RGB stars of their sample (low C and Li and high N abundances, and low $^{12}C/^{13}C$ ratio). Thus, the general abundance patterns of mixed RGB and HB/AGB stars are rather similar.

#### 4.3.1. The Na and Al anomalies

During the evolution of moderately metal-poor stars ([Fe/H] > −2.0) in the field, from the main sequence to the top of the RGB, Gratton et al. (2000) have not detected any variation of [Na/Fe], as can be seen from inspection of their Fig. 7.

In AGB stars with very low metallicity ($Z = 10^{-5}$), the temperatures are higher, and rotationally-induced deep-mixing episodes are expected to occur (Meynet & Maeder 2002; Herwig 2005), which can affect the atmospheric Na and Al abundances. Proton capture converts C and O into N, but also Ne into Na and Mg into Al. However, proton capture on Mg requires temperatures which are generally considered as too high for being reached in RGB stars. Following Weiss & Charbonnel (2004), Al anomalies would be a likely signature of AGB stars.

Figure 8 shows the observed [Na/Mg] and [Al/Mg] ratios vs. [Fe/H]. No corrections for NLTE effects have been applied; while Baumüller et al. (1997, 1998) estimate that they could reach –0.5 dex for Na and +0.6 dex for Al, Gratton et al. (1999) find a value of only –0.1 dex for Na.

Defining mean relations for the unmixed stars in Figs. 8a,b (dashed lines), we can compute individual Na and Al excesses Δ[Na/Mg] and Δ[Al/Mg] for all our stars. These are shown in Fig. 9 as functions of [C/N]. Because [Na/Mg] increases with [Fe/H] (Fig. 8a) and because there are no unmixed giants above [Fe/H] > −2.6 in our sample, we cannot compute mean values of [Na/Mg] and corresponding Na and Al excesses for [Fe/H] > −2.6. Thus, the most metal-rich stars in our sample are not included in Fig. 9.

The mixed stars have slightly higher Na and Al excesses than the unmixed stars. Three stars with [Fe/H] < −2.6 are both Na- and Al-rich, and all three are mixed stars (Figs. 8 and 9): CS 22873-55, CS 22891-209, and CS 22952-15. These three stars all have low [C/N] ratios ([C/N] < −1.6); CS 22952-015 has the lowest [C/N] ratio of them all and is also Mg-poor, as expected if Mg-Al cycling has played an important role.

In summary, the evidence suggesting that the Na- and Al-rich stars are in fact AGB stars are:

- the observed Na and especially Al enrichment requires mixing with very deep high-temperature layers, which is not predicted to occur in RGB stars;
- the Na-Al-rich stars are located above the theoretical RGB isochrone (Fig. 5).

Note that the most metal-rich star of our sample in Fig. 8 is a mixed star: BD + 17°3248 ([Fe/H] = −2.07). Following the measurements of Johnson (2002), the relations [Na/Mg] and [Al/Mg] vs. [Fe/H] are flat for −2.5 < [Fe/H] < −2.0 and thus

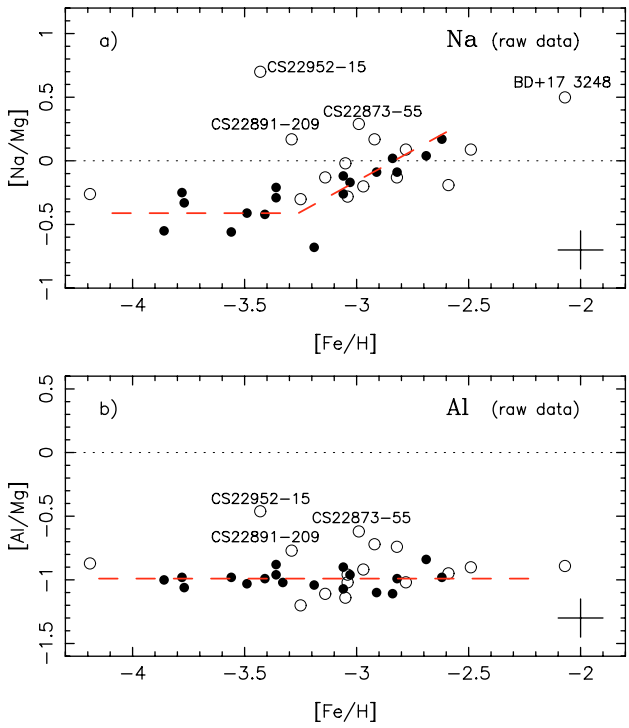


**Fig. 8.** [Na/Mg] and [Al/Mg] (without NLTE corrections, hereabove "'raw data") vs. [Fe/H]; symbols as in Fig. 2. At low metallicity ([Fe/H] < −2.6) all the Na-rich stars are mixed; they are also Al-rich and located above the theoretical isochrone in the H-R diagram (Fig. 5), suggesting that they belong to the AGB. The dashed lines represent the mean value of the relations for the unmixed stars alone. The scatter in [Al/Mg] for these stars alone is $\sigma_{[Al/Mg]} = 0.07$ dex, consistent with the measurement errors; thus, any cosmic scatter is below our detection limit.

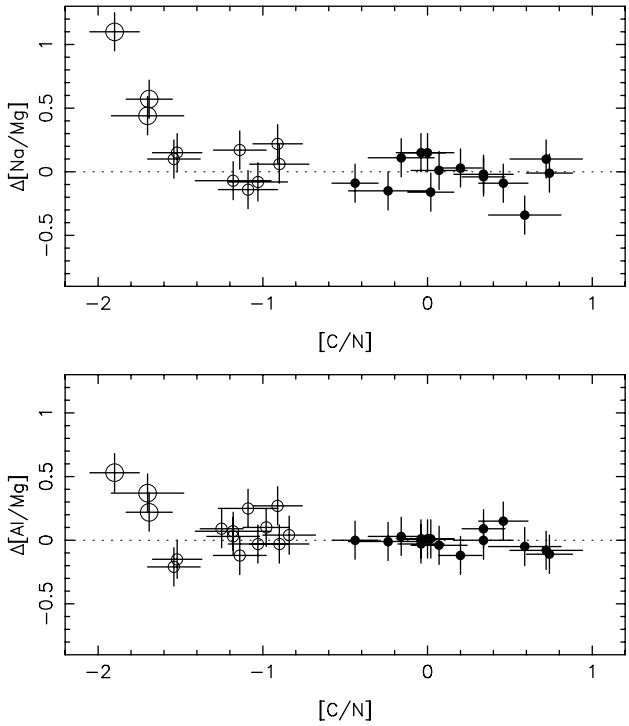


**Fig. 9.** Na and Al excesses, Δ[Na/Mg] and Δ[Al/Mg], relative to the relations shown by dashed lines in Fig. 8, vs. [C/N], for [Fe/H] < −2.6; symbols as in Fig. 8. The large open circles denote the three Na- and Al-rich stars from Fig. 8; these stars also have the lowest C/N ratios.

BD + 17°3248 could also be Na-rich. Its aluminum abundance seems to be normal. At log $L/L_\odot = 2.80$ and $T_{\rm eff} = 5250$ K, this star is far above the isochrones in Fig. 5, and could thus also be an AGB star, as already claimed by Bond (1980) and Johnson (2002). However, note that its [C/N] ratio, while low ([C/N] = −0.98), is not extreme.

Unlike most AGB stars, the three Na-rich EMP stars in our sample are not enriched in *s*-elements such as Sr or Ba (François et al., 2006, "First Stars VIII"). According to Cowan et al. (2002), BD + 17°3248 is very rich in neutron-capture elements, but these seem to have been produced by the *r*-process, probably during an earlier supernova explosion, not in the star itself. The *s*-element production in AGB stars occurs quite late in the AGB phase, after the start of thermal pulses; thus, we would not expect to see an enhancement of these elements if the observed stars are in the early AGB phase.

However, alternative interpretations of the Al and Na excesses are possible, in particular when one takes into account the fact that the temperatures needed in particular to transform Mg into Al are encountered only in AGB stars; e.g.:

- mass transfer from a former, more massive AGB binary companion, which has now evolved into a white dwarf. It would be very interesting to monitor the radial velocities of these stars to check this hypothesis;
- inhomogeneous enrichment of the ISM by a previous generation of AGB stars.

Finally, it is interesting to note that the mean value of [Al/Mg] over all stars (Fig. 8b) is $\langle$[Al/Mg]$\rangle = -0.95 \pm 0.15$ (s.d.), but the scatter drops by a factor two if *only the unmixed stars* are considered: $\langle$[Al/Mg]$\rangle = -0.99 \pm 0.07$ (no NLTE corrections).

A similar trend is seen for Na, but $\langle$[Na/Mg]$\rangle$ only becomes constant below [Fe/H] = −3.2, and the scatter remains higher than for Al (Fig. 8a).

#### 4.3.2. Are signatures of the ON cycle visible in the mixed stars?

Because we seem to observe products of the Ne-Na and Mg-Al cycles in some stars, we might expect products of the ON cycle to be directly observable as well, since the ON cycle occurs at about the same temperature as the NeNa chain (e.g. Weiss & Charbonnel 2004).

Our earlier plot of [O/Fe] vs. [Fe/H] ("First Stars VI", Fig. 10) showed no significant difference between mixed and unmixed stars. Thus, we concluded that mixing with ON-cycled material is not efficient. However, the absolute abundance (i.e., number of atoms per $10^{12}$ H atoms) is much larger for O than for N; thus, a decrease in O due to ON cycling could exist, but might not be detected in [O/Fe] or [O/Mg] due to their rather large observational errors. Indeed, a plot of [(C+N)/Fe] vs. [Fe/H] (Fig. 10) seems to show that, in the mean, the mixed stars have a C+N excess which could be due to N produced by the ON cycle.

In the red giants of M 5, an increase of C+N with decreasing C was also observed by Cohen et al. (2002), and interpreted as the result of an admixture of ON-processed material to the surface layers. However, prudence is advisable in interpreting the [(C+N)/Fe] excess in our mixed stars. Because the N abundances of the mixed and unmixed stars differ by almost a factor of ten, the total number of C+N atoms is close to the number of C atoms alone in the unmixed stars, and to the number of N atoms in the mixed stars. Therefore, slight systematic errors in the C or N abundance determinations (NLTE, 3D...) could produce the observed effect.

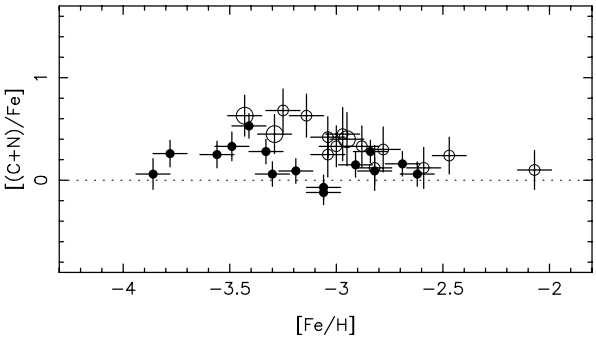


**Fig. 10.** [(C+N)/Fe] vs. [Fe/H]; symbols as in Fig. 8. The three large open circles indicate the three Na- and Al-rich stars. The C+N excess of the mixed stars could be due to the ON cycle.

For example, we recall that N abundances derived from the NH band needed a correction of 0.4 dex to reconcile them with those from the CN band ("First Stars VI"). Had we instead adopted a correction of, say, 0.8 dex, the mean value of [(C+N)/Fe] would be the same in the mixed and unmixed stars, and there would be no indication of any ON cycling.

We can also compare the scatter in the relations of [(C+N)/Fe] vs. [Fe/H] and [(C+N+O)/Fe] vs. [Fe/H]. If ON-processed material has been mixed to the surface in some stars, the first relation should exhibit larger scatter than the second one. However, first, the number of stars with [(C+N+O)/Fe] is smaller (O could be measured in only 23 stars, two of them being peculiar C-rich stars). Secondly, because O is more abundant than C and N, the dispersion in [(C+N+O)/Fe] is mainly due to the uncertainty of the O abundance, which is large because the [O I] line is very weak. Definite conclusions on the presence of ON cycled matter cannot be drawn from the scatter in these two relations.

Finally, if the chemical composition of the atmosphere of some giants has been affected by the ON cycle, we could expect a relation between [O/Fe] and Na excess. This anticorrelation is observed both on the RGB and in turnoff and subgiant stars of some globular clusters (e.g., Gratton et al. 2004). The best explanation of the anomalies seen in globular clusters is that proton capture converted C and O into N and Ne into Na, either

- in the H burning shell of the star itself, followed by convection (not expected in giants, and impossible in turnoff or subgiant stars);
- or in a previous stellar generation which enriched the ISM inhomogeneously;
- or in a former AGB binary companion, which polluted the atmosphere of the observed star through stellar winds.

Figure 11 shows Δ[Na/Fe] as a function of [O/Fe], where Δ[Na/Fe] is the Na excess relative to the average [Na/Fe] for the [Fe/H] of the star (analogous to Fig. 9, but for [Na/Fe] instead of [Na/Mg]). No significant anticorrelation between Δ[Na/Fe] and [O/Fe] is seen within the measurement errors. The two Na-rich stars in the figure, CS 22873-055 and CS 22891-209 (see also Fig. 8), are probably AGB stars. We have been unable to measure O in the third Na-rich star, CS 22952-015, because its radial velocity is small and the stellar [O I] line is obliterated by a saturated sky emission line.

In summary, we cannot prove that an O-Na anticorrelation exists in the mixed EMP giants, and thus have no clear evidence from this relation that the ON cycle has been active. However, because the Ne-Na and Mg-Al cycles operate at the same or even

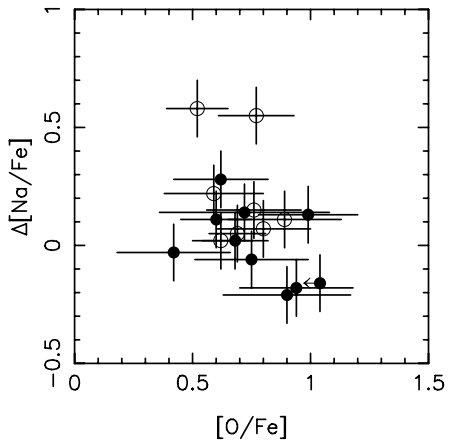


**Fig. 11.** Δ [Na/Fe] vs. [O/Fe]; symbols as in Fig. 3. Δ [Na/Fe] is the Na excess relative to ⟨[Na/Fe]⟩ at the [Fe/H] of the star. There is no obvious correlation between Na excess and [O/Fe].

a higher temperatures than the ON cycle (Weiss & Charbonnel 2004), and we do find Na and Al enhancements in a few stars, it is likely that the ON cycle has polluted the atmosphere of at least these few mixed stars.

## 5. Conclusions

We have analysed new $^{12}C/^{13}C$ isotopic ratios for a sample of 35 EMP red giants, including 22 stars with [Fe/H] $\leqslant -3.0$, and find the following new results:

- Clear (anti)correlations exist between $^{12}C/^{13}C$ and [N/Fe] and [C/Fe], as expected if the C and N abundances are modified by admixtures of CNO-processed material. However, there seem to be large variations in the C and N abundance of the near-primordial ISM from which these stars formed; many EMP stars are C-rich and some are N-rich, so the C/N ratio is not a clean indicator of internal mixing. The $^{12}C/^{13}C$ ratio is a much better diagnostic, because $^{12}C/^{13}C$ should be high in primordial matter ($> 70$) and its determination is insensitive to the choice of atmospheric parameters for the stars.
- The depletion of Li is the first observational signature of mixing, because it occurs in shallower layers than the CNO cycle; therefore, it is a useful complement to the C and N results which were used in "First stars VI" to separate our sample into "mixed" and "unmixed" stars. In the lower RGB stars, we find a narrow correlation between $^{12}C/^{13}C$ and $A$(Li); in the more evolved (mixed) stars, $\log {}^{12}C/^{13}C \approx 0.7$ and Li ($A(\mathrm{Li}) < -0.1$) is not detected, and is likely to have been destroyed.
- Computing luminosities from $T_{\rm eff}$ and log g allows us to place the stars in the H-R diagram. For the RGB stars, we find a good fit between the observations and 14 Gyr isochrones by Kim et al. (2002) for the appropriate chemical composition. Interestingly a few mixed stars fall somewhat above the isochrone, suggesting an AGB phase.
- The main signatures of deep mixing are a low $^{12}C/^{13}C$ ratio, a low Li abundance, and a high N abundance ($^{12}C/^{13}C < 10$, $\log A(\mathrm{Li}) < 0.0$, and [N/Fe] $> 0.5$). These appear above a luminosity of $\log L/L_\odot = 2.6$. This is higher than the luminosity at which extra mixing was found in less metal-poor stars by Gratton et al. (2000): $\log L/L_\odot = 2.0$. However in both samples this limit of deep mixing corresponds to the luminosity of the bump.
- At variance with the suggestion of Gratton et al. (2000) we did not find that the extra mixing decreases in stars below [Fe/H] $\approx -1.5$.
- Assuming that our mixed EMP stars are evolving along the RGB, we find that extra mixing sets in when a star crosses the bump in the luminosity function. As soon as this happens, the $^{12}C/^{13}C$ ratio decreases very rapidly, both in EMP and in moderately metal-poor stars. Standard models that include only convection can explain neither this observation nor the depletion of Li at low temperature or high luminosity.
  - Our results about $^{12}C/^{13}C$ are consistent with the rotating models by Chanamé et al. (2005) for globular-cluster stars, but only for very fast turnoff rotation rates ($V_{\rm TO} > 70$ km s$^{-1}$). Because metal-poor field turnoff stars have $v \sin i < 10$ km s$^{-1}$, rotation is probably not the only cause of extra mixing in RGB stars, but it would be important to check this directly with models for EMP stars ([Fe/H] $< -3$).
  - Our lithium measurements agree neither with the models of Delyannis and Charbonnel (as reported by Garciá Pérez & Primas 2006) nor with the models of Palacios et al. (2006).
- As an alternative interpretation, at least some of our mixed stars could be early AGB stars, with the core helium flash driving additional mixing processes. Overall, there are no striking abundance differences between mixed RGB stars and AGB stars, but the Na and Al abundances offer useful clues. For the first time in metal-poor field giants, we find several of our mixed stars to be Na- and Al-rich, suggesting that a deep-mixing episode has taken place. This is sometimes expected to occur in AGB stars (Herwig 2005), but Al enhancement seems to be impossible in RGB stars, even with extra mixing (e.g. Weiss & Charbonnel 2004). The Na- and Al-rich giants generally lie above the theoretical RGB, suggesting that they may indeed be AGB stars. However, it remains possible that the Na and Al (and N) enrichment could be due to inhomogeneous enrichment of the ISM by a previous generation of stars, or to pollution by a former AGB binary companion.
- The scatter of [Al/Mg] around its mean value for the unmixed stars alone is extremely low: $\sigma = 0.07$ dex, corresponding to the measurement errors alone (see "First Stars V"). The mean value of [Al/Mg] in the pristine ISM appears to be [Al/Mg] $\approx -0.39$ (applying an NLTE correction of +0.6 dex), with negligible cosmic scatter.
- Because the Ne-Na and Mg-Al cycles seem to have influenced some of our stars, we would expect that signs of the ON cycle should also be visible in at least these stars. It does indeed seem that, on average, [(C+N)/Fe] is larger in the mixed stars than in the unmixed stars. However, this could perhaps be due to slight systematic errors in the C or N abundances (e.g., from NLTE or 3D effects).

Understanding the abundances of light elements such as C, N, O, Na, and Al and their scatter in the pristine ISM remains an important goal for the future. In order to make progress from abundance analyses of EMP giants, it is crucial to understand what mixing processes may have affected their atmospheres. Dwarf and turnoff stars are free from such mixing, but measuring N abundances in EMP dwarfs is practically impossible, because even the near-UV band of NH is too weak unless the stars are actually N rich. Thus, EMP giants will remain a key source of data in the foreseeable future, and the lines of analysis presented will need further refinement.

For this to become possible, more accurate laboratory data for the NH and CN bands, in particular, are badly needed. NLTE 3D computations are the next crucial step. Precise trigonometric parallaxes for EMP giants (from SIM or GAIA) will be essential in order to distinguish RGB and AGB stars. Finally, the radial velocities of the mixed giants should be monitored to assess the frequency of binaries among them, and thus whether the observed abundance anomalies could originate in a companion star that has gone through the AGB stage in the past.

*Acknowledgements.* We thank the ESO staff for assistance during all the runs of our Large Programme. RC, PF, VH, BP, FS and MS thank the PNPS and the PNG for their support. PB and PM acknowledge support from the MIUR/PRIN 2004025729_002 and PB from EU contract MEXT-CT-2004-014265 (CIFIST). T.C.B. acknowledges partial funding for this work from grants AST 00-98508, AST 00-98549, and AST 04-06784 as well as from grant PHY 02-16783: Physics Frontiers Center/Joint Institute for Nuclear Astrophysics (JINA), all from the U.S. National Science Foundation. BN and JA thank the Carlsberg Foundation and the Swedish and Danish Natural Science Research Councils for partial financial support of this work.

## References

Alonso, A., Arribas, S., & Martínez-Roger, C. 1999, A&AS, 140, 261
Alvarez, R., & Plez, B. 1998, A&A, 330, 1109
Ballester, P., Modigliani, A., Boitiquin, O., et al. 2000, ESO Messenger, 101, 31
Baumüller, D., & Gehren, T. 1997, A&A, 325, 1088
Baumüller, D., Butler, K., & Gehren, T. 1998, A&A, 338, 637
Bellman, S., Briley, M. M., Smith, G. H., & Claver, C. F. 2001, PASP, 113, 326
Bond, H. E. 1980, ApJS, 44, 517
Bonifacio, P., Molaro, P., Sivarani, T., et al. 2006, A&A, submitted ("First Stars VII")
Boothroyd, A. I., & Sackmann, I.-J., 1999, ApJ, 510, 232
Cayrel, R., Depagne, E., Spite, M., et al. 2004, A&A, 416, 1117 ("First Stars V")
Chanamé, J., Pinsonneault, M., & Terndrup, D. 2005, ApJ, 631, 540
Charbonnel, C. 1994, A&A, 282, 811
Charbonnel, C. 1995, ApJ, 453, L41
Charbonnel, C., Brown, J. A., & Wallerstein, G. 1998, A&A, 332, 204
Cohen, J. G., Briley, M. M., & Stetson, P. B. 2002, ApJ, 123, 2525
Cowan, J. J., Sneden, C., Burles, S., et al. 2002, ApJ 512, 861
Dekker, H., D'Odorico, S., Kaufer, A., et al. 2000 in Optical and IR Telescopes Instrumentation and Detectors, ed I. Masanori, & A.F. Morwood Proc. SPIE, 4008, 534
Denissenkov, P. A., & VandenBerg, D. A. 2003, ApJ, 593, 509
Denissenkov, P. A., & Weiss, A. 2004, ApJ, 603, 119
Depagne, E., Hill, V., Spite, M., et al. 2002, A&A, 390, 187 ("First Stars II")
François, P., Depagne, E., Hill, V., et al. 2006, A&A, in preparation ("First Stars VIII")
García Pérez, A. E., & Primas, F. 2006, A&A, 447, 299
Gilroy, K. K. 1989, ApJ, 347, 835
Gratton, R., Carretta, E., Eriksson, K., & Gustafsson, B. 1999, A&A, 350, 955
Gratton, R., Sneden, C., Carretta, E., & Bragaglia, A. 2000, A&A, 354, 169
Gratton, R., Sneden, C., & Carretta, E. 2004, ARA&A, 42, 385
Grundahl, F., Briley, M., Nissen, P. E., & Feltzing, S. 2002, A&A, 385, L14
Gustafsson, B., Bell, R. A., Eriksson, K., & Nordlund, Å. 1975, A&A, 42, 407
Gustafsson, B., Edvardsson, B., Eriksson, K., et al. 2003 in Stellar Atmosphere Modeling, ed. I. Hubeny, D. Mihalas, & K. Werner, ASP Conf. Ser., 288 331
Herwig, F. 2005, ARA&A, 43, 435
Hill, V., Plez, B., Cayrel, C., et al. 2002, A&A, 387, 560 ("First Stars I")
Houdashelt, M. L., Bell, R. A., & Sweigart, A. V. 2000, AJ, 119, 1448
Jacobson, H. R., Pilachowski, C. A., & Friel, E. D. 2005, Bull. AAS, 37, 1280
Johnson, J. A. 2002, ApJ, 139, 219
Jørgensen, U. G., Larsson, M., Iwamae, A., & Yu, B. 1996, A&A, 315, 204
Keller, L. D., Pilachowski, C. A., & Sneden, C. 2001, AJ, 122, 2554
Kim, Y.-C., Demarque, P., Yi, S. K., & Alexander D. R. 2002, ApJS, 143, 499
Kraft, R. P. 1994, PASP, 106, 553
Levshakov, S. A., Centurion, M., Molaro, P., & Kostina, M. V. 2006, A&A, 447, L21
Lucatello, S., & Gratton, R. G. 2003, A&A, 406, 691
Luque, J., & Crosley D. R. 1999, SRI Int. Rep. MP 99-099
Meléndez, J., Shchukina, N. G., Vasiljeva, I. E., & Ramirez, I. 2006, ApJ, 642, 1082
Meynet, G., & Maeder, A. 2002, A&A, 390, 561
Palacios, A., Charbonnel, C., Talon, S., & Siess, L. 2006, [arXiv:astro.ph.0602389]
Plez, B., Hill, V., Cayrel, R., et al. 2004, ApJ, 617, L119
Shetrone, M. D. 2003 ApJ, 585, L45
Shetrone, M. D., Sneden, C., & Pilachowski, C. A. 1993, PASP, 105, 337
Sneden, C., Pilachowski, C. A., & VandenBerg, D. A. 1986, AJ, 311, 826
Sneden, C., Cowan, J. J., Ivans, I. I., et al. 2000, ApJ, 533, L139
Sneden, C., Cowan, J. J., Lawler, J. E., et al. 2003, ApJ, 591, 936
Spite, M., Cayrel, R., Plez, B., et al. 2005, A&A, 430, 655 ("First Stars VI")
Weiss, A., & Charbonnel, C. 2004, MmSAI, 75, 347